molecular microbiology

Overexpression of SepJ alters septal morphology and heterocyst pattern regulated by diffusible signals in Anabaena

Journal:	*Molecular Microbiology*
Manuscript ID	MMI-2016-15872.R1
Manuscript Type:	Research Article
Date Submitted by the Author:	n/a
Complete List of Authors:	Mariscal, Vicente; CSIC, Instituto de Bioquimica Vegetal y Fotosintesis Nuernberg, Dennis; Queen Mary University of London, School of Biological and Chemical Sciences; Imperial College London, Department of Life Sciences Herrero, Antonia; Consejo Superior de Investigaciones Científicas, Instituto de Bioquímica Vegetal y Fotosíntesis; Mullineaux, Conrad; Queen Mary University of London, School of Biological and Chemical Sciences Flores, Enrique; CSIC, Instituto de Bioquimica Vegetal y Fotosintesis
Key Words:	Bacterial development, Cyanobacteria, Heterocyst differentiation, Intercellular communication, Morphogen

Overexpression of SepJ alters septal morphology and heterocyst pattern regulated by diffusible signals in *Anabaena*

Vicente Mariscal[1], Dennis J. Nürnberg[2#], Antonia Herrero[1], Conrad W. Mullineaux[2] and Enrique Flores[1,*]

[1]*Instituto de Bioquímica Vegetal y Fotosíntesis, Consejo Superior de Investigaciones Científicas and Universidad de Sevilla, Américo Vespucio 49, E-41092 Seville, Spain, and* [2]*School of Biological and Chemical Sciences, Queen Mary University of London, London E1 4NS United Kingdom.*

[#]Current address: Department of Life Sciences, Imperial College London, London SW7 2AZ, United Kingdom

*For correspondence. Tel.: +34954489523; E-mail: eflores@ibvf.csic.es.

Running title: SepJ overexpression in *Anabaena*

Key words: Bacterial development; Cyanobacteria; Heterocyst differentiation; Intercellular communication.

Summary

Filamentous, N_2-fixing, heterocyst-forming cyanobacteria grow as chains of cells that are connected by septal junctions. In the model organism *Anabaena* sp. strain PCC 7120, the septal protein SepJ is required for filament integrity, normal intercellular molecular exchange, heterocyst differentiation and diazotrophic growth. An *Anabaena* strain overexpressing SepJ made wider septa between vegetative cells than the wild type, which correlated with a more spread location of SepJ in the septa as observed with a SepJ-GFP fusion, and contained an increased number of nanopores, the septal peptidoglycan perforations that likely accommodate septal junctions. The septa between heterocysts and vegetative cells, which are narrow in wild-type *Anabaena*, were notably enlarged in the SepJ-overexpressing mutant. Intercellular molecular exchange tested with fluorescent tracers was increased for the SepJ-overexpressing strain specifically in the case of calcein transfer between vegetative cells and heterocysts. These results support an association between calcein transfer, SepJ-related septal junctions and septal peptidoglycan nanopores. Under nitrogen deprivation, the SepJ-overexpressing strain produced an increased number of contiguous heterocysts but a decreased percentage of total heterocysts. These effects were lost or altered in *patS* and *hetN* mutant backgrounds, supporting a role of SepJ in the intercellular transfer of regulatory signals for heterocyst differentiation.

Introduction

Filamentous cyanobacteria of the order Nostocales fix dinitrogen in specialized cells called heterocysts, which are found with a spaced pattern of about one heterocyst per ten vegetative photosynthetic cells along the filament (Flores and Herrero, 2010). Heterocysts are formed from vegetative cells when the organism has no source of

combined nitrogen available (Wolk, 1996). It was proposed that, to attain such spacing, heterocysts or prospective heterocysts (proheterocysts) produce a diffusible inhibitor to prevent the differentiation of neighboring cells into heterocysts (Wilcox *et al.*, 1973; Wolk and Quine, 1976). The *patS* gene encoding a polypeptide of 17 amino acids that appears to be processed to produce a smaller peptide that inhibits heterocyst differentiation (Yoon and Golden, 1998, 2001; Corrales-Guerrero *et al.*, 2013) has been identified in the model heterocyst-forming cyanobacterium *Anabaena* sp. strain PCC 7120 (hereafter *Anabaena* or wild type [WT]). A synthetic peptide, known as PatS-5, corresponding to the five C-terminal amino acids of PatS (RGSGR) inhibits heterocyst differentiation when added to cultures of *Anabaena*, suggesting that it could be the inhibitor (Yoon and Golden, 1998, 2001). More recent work has shown, however, that the active inhibitor could correspond to a product consisting of the eight C-terminal amino acids of PatS (Corrales-Guerrero *et al.*, 2013). In *Anabaena*, the *hetN* gene encodes a 287-amino acid protein that somehow inhibits heterocyst differentiation and contains an internal ERGSGR sequence (amino acid residues 131 to 136), which is common to the six C-terminal residues of PatS (Callahan and Buikema, 2001; Higa *et al.*, 2012; Corrales-Guerrero *et al.*, 2014a). This internal sequence is needed for HetN to produce inhibition of hetererocyst differentiation, implying that in *Anabaena* HetN might produce a regulator similar to PatS (Higa *et al.*, 2012; Corrales-Guerrero *et al.*, 2014a). Nonetheless, the PatS-like internal sequence is found only in HetN from a few heterocyst-forming cyanobacteria related to *Anabaena*, and HetN appears to have an additional role in heterocyst biology (Corrales-Guerrero *et al.*, 2014a).

Heterocyst differentiation in response to nitrogen deficiency requires two main transcription factors, the global regulator NtcA, which promotes gene expression under high carbon-to-nitrogen balance cellular conditions, and the differentiation-specific

HetR protein (Kumar *et al.*, 2010; Herrero *et al.*, 2013). Inhibition of heterocyst differentiation by PatS- and possible HetN-derived products appears to involve inhibition of HetR (Khudyakov and Golden, 2004), and the binding to HetR of different peptides corresponding to C-terminal sequences of PatS has been described (Feldmann *et al.*, 2011, 2012). Indeed, PatS-5 inhibits a DNA-binding activity of HetR (Huang *et al.*, 2004; Valladares *et al.*, 2016). The PatS- and possible HetN-derived products active in inhibition of heterocyst differentiation would be transferred from the producing cells to their neighbors (Yoon and Golden, 1998), where they have been suggested to promote degradation of HetR (Risser and Callahan, 2009). Material reacting with antibodies raised against PatS-5 has been detected in cells proximal to *patS*-producing proheterocysts, but not in the proheterocysts, consistent with the intercellular transfer of a PatS-derived morphogen (Corrales-Guerrero *et al.*, 2013). The mechanism of transfer is however unknown, although recent data has suggested the involvement of the ABC transporter HetC in export of PatS from the heterocysts (Corrales-Guerrero *et al.*, 2014b; Videau *et al.*, 2015).

Cyanobacteria bear a Gram-negative type of cell envelope (Han and Schleiff, 2014). In filamentous cyanobacteria, whereas each cell is surrounded by its cytoplasmic membrane and peptidoglycan layer(s), the outer membrane is continuous along the filament (reviewed in Han and Schleiff, 2014). Cells in the filament appear to be joined by septal junctions (Mariscal, 2014; Mullineaux and Nürnberg, 2014; Flores *et al.*, 2016), previously known as microplasmodesmata or septosomes (Lang and Fay, 1971; Giddings and Staehelin, 1978, 1981; Wilk *et al.*, 2011). These structures traverse the septal peptidoglycan layers through perforations (termed nanopores or channels) that are visible by transmission electron microscopy of whole filaments (Wilk *et al.*, 2011) or isolated murein sacculi (Lehner *et al.*, 2013), or by electron tomography of whole

filaments (Omairi-Nasser *et al.*, 2014). Proteins that contribute to the formation of septal junctions in *Anabaena* include SepJ (also known as FraG; Nayar *et al.*, 2007), FraC and FraD (Flores *et al.*, 2007; Merino-Puerto *et al.*, 2010; Nürnberg *et al.*, 2015). Fluorescent tracers, calcein, 5-carboxyfluorescein (5-CF) and the sucrose analogue esculin, have been used to probe intercellular molecular exchange in heterocyst-forming cyanobacteria (Mullineaux *et al.*, 2008; Lehner *et al.*, 2011; Mariscal *et al.*, 2011; Nürnberg *et al.*, 2015). The molecular mass of the largest of the tested fluorescent tracers, calcein, is 622 Da, similar to that of the PatS-5 peptide (532 Da) or of a peptide made of the last eight amino acids of PatS (879 Da). However, calcein is different from these peptides regarding chemical structure and charge, calcein being negatively charged and the PatS peptides being positively charged. *Anabaena* mutants with *sepJ* and *fraC-fraD* deleted show a decreased number of septal peptidoglycan perforations (Nürnberg *et al.*, 2015) and are impaired in the intercellular transfer of those tracers, but whereas *fraC* and *fraD* deletion mutants are generally impaired in the transfer of the three tracers, a *sepJ* deletion mutant is significantly more affected in the transfer of calcein than of 5-CF (Mariscal *et al.*, 2011; Merino-Puerto *et al.*, 2011; Nürnberg *et al.*, 2015). Two types of septal junctions may therefore be present in *Anabaena*, one related to SepJ and another related to FraC and FraD (Merino-Puerto *et al.*, 2011).

Based on expression of *patS* or *hetN* from a plasmid in vegetative cells and its effect on HetR stability in some mutant backgrounds, it has been suggested that SepJ is involved in intercellular transfer of a HetN-derived signal but not of a PatS-derived regulator (Rivers *et al.*, 2014). On the other hand, in a study of the expression of a *hetR-gfp* fusion along the cells in *Anabaena* filaments, the pattern of expression (in ammonium-grown filaments or in filaments incubated for short times in the absence of combined nitrogen) was observed to be altered in *patS* and *sepJ* deletion mutants

suggesting a relation between the products of these genes in the regulation of *hetR* expression (Corrales-Guerrero *et al.*, 2015). In contrast, no evidence was found in that study for a specific relation of HetN to SepJ. To explore further the possible roles of SepJ in heterocyst-forming cyanobacteria, we introduced a *sepJ* overexpression construct in several *Anabaena* mutant backgrounds. The results obtained support a role of SepJ in the formation of septal peptidoglycan nanopores and in septal morphology, as well as in the distribution of the PatS morphogen and, possibly, of a HetN-dependent regulator of heterocyst differentiation along the *Anabaena* filament.

Results

Anabaena *strains overexpressing SepJ*

Mutation of *sepJ* in *Anabaena* causes a pleiotropic phenotype including filament fragmentation, impaired intercellular transfer of calcein, a decrease in the number of septal peptidoglycan nanopores, and an early arrest of heterocyst differentiation (Nayar *et al.*, 2007; Flores *et al.*, 2007; Mullineaux *et al.*, 2008; Mariscal *et al.*, 2011; Nürnberg *et al.*, 2015). To gain further insights into the role of SepJ in multicellularity and heterocyst differentiation, we sought the construction of *Anabaena* strains with an increased expression of the *sepJ* gene as compared to the wild-type. For this purpose, the *sepJ* open reading frame was cloned in a replicative plasmid next to the C.K1 gene cassette, which can be used to promote gene expression (see e.g. Vázquez-Bermúdez *et al.*, 2000). The gene cassette was inserted in both orientations with respect to *sepJ* (Fig. 1A), and the SepJ protein was detected by western blot analysis in *Anabaena* and strains carrying these plasmids (Fig. 1B). Strain CSDN2a carrying the plasmid bearing the C.K1 gene cassette and the *sepJ* gene in the same orientation showed 4.1 ± 1.4 (mean ±

SEM; n = 3)-fold higher levels of SepJ than the wild type. Strain CSDN2b carrying the plasmid bearing the C.K1 gene cassette in opposite orientation to *sepJ* showed about 2.3-fold higher levels of SepJ than the wild type (Fig. 1B). The increased SepJ levels in strain CSDN2b may correspond to the added expression of the *sepJ* chromosomal copy and of the *sepJ* copy in the plasmid (which however lacked a specific promoter). The increased SepJ levels in strain CSDN2a should result from the added expression of the chromosomal and plasmid copies of *sepJ*, the latter expressed from the *npt* gene promoter in the C.K1 gene cassette. Strain CSDN2a (which is *Anabaena* carrying the replicative plasmid pCSDN2a that bears the C.K1-*sepJ* construct) was further characterized. For simplicity, it will be referred to as WT+pSepJ.

Strain WT+pSepJ could grow on solid medium with (BG11) or without ($BG11_0$) combined nitrogen, although some impairment of growth was observed in $BG11_0$ medium (Fig. 2A). Growth in liquid medium was also tested as described in Experimental procedures. In BG11 medium, similar growth rate constants were determined for *Anabaena* and WT+pSepJ, $\mu = 0.62 \pm 0.06$ day^{-1} and 0.63 ± 0.02 day^{-1}, respectively (mean ± SD, three independent cultures in each case). In $BG11_0$ medium, the growth rate of the SepJ overexpressing strain was lower than that of the wild type, $\mu = 0.39 \pm 0.02$ day^{-1} and 0.17 ± 0.03 day^{-1} for *Anabaena* and WT+pSepJ, respectively (mean ± SD, n = 3; Student's *t* test $p = 0.001$). Microscopic inspection showed the presence of normal, long filaments in the liquid cultures of WT+pSepJ (Fig. 2B). Nitrogenase activity (acetylene reduction) was determined in filaments that had been incubated for 48 in liquid $BG11_0$ medium. Acetylene reduction assays were carried out under oxic and anoxic conditions as previously described (Burnat *et al.*, 2014). Under oxic conditions, the activity of WT+pSepJ was about 7 % the wild-type activity (0.64 ± 0.36 vs. 8.67 ± 1.45 μmol ethylene produced $(mg\ Chl)^{-1}\ h^{-1}$). Assay under anoxic

conditions increased nitrogenase activity about twice both in the mutant and in the wild type (1.30 ± 0.37 and 19.69 ± 1.47 μmol (mg Chl)$^{-1}$ h^{-1}, respectively).

Filament structure in strain WT+pSepJ

The structure of WT+pSepJ was studied by electron microscopy and compared to wild-type *Anabaena*. Heterocysts from WT+pSepJ showed an unusually wide heterocyst neck, which was observed in all the heterocysts that could be visualized (three specimens shown in Fig. 3; compare with the neck of heterocysts from *Anabaena* in Fig. 3 and in, e.g., Flores *et al.*, 2007, 2016; Kumar *et al.*, 2010; Omairi-Nasser *et al.*, 2014). The wide heterocyst neck implies the presence of a wide heterocyst-vegetative cell septum (Fig. 3). Although not observed in specimens A and B, the cyanophycin plug present in the heterocyst necks in *Anabaena* could also be found in some heterocysts from WT+pSepJ (Fig. 3, specimen C). In contrast, no alterations could be noted in the septa between vegetative cells.

To look further into the septa between vegetative cells and between heterocysts and vegetative cells, we performed labeling with a fluorescently labeled derivative of vancomycin, Van-FL, which binds to regions of the cell that are actively synthesizing peptidoglycan (Daniel and Errington, 2003; Tiyanont *et al.*, 2006; Lehner *et al.*, 2013) and labels well the intercellular septa in *Anabaena* (see, e.g., Burnat *et al.*, 2014). Van-FL fluorescence was readily observed between vegetative cells of both *Anabaena* and WT+pSepJ (Fig. 4A). Quantification of septal width based on Van-FL labeling revealed the presence of wider septa in WT+pSepJ than in the wild type for BG11-grown filaments (about 1.18-fold wider) and filaments incubated in $BG11_0$ medium (about 1.24- and 1.36-fold wider at 24 and 48 h after nitrogen deprivation, respectively; Fig. 5). It should be noted that the increase in septal width observed under the microscope

196 corresponds to a larger increase (1.4- to 1.9-fold) in septal disk area. We also looked
197 into the heterocyst-vegetative cell septa. At 24 h (Fig. 4A), septal width was 0.53 ± 0.11
198 nm and 1.30 ± 0.53 nm for the wild type and WT+pSepJ, respectively (Student *t* test p =
199 0.01), and at 48 h (not shown), 0.60 ± 0.07 nm and 1.10 ± 0.30 nm for the wild type and
200 WT+pSepJ, respectively (Student *t* test p = 0.002). Thus, based on Van-FL labeling,
201 heterocyst-vegetative cell septa in the SepJ-overexpressing mutant were about twice the
202 width (and about 3.4- to 6-fold the area) in the wild type. The larger difference between
203 mutant and wild type in heterocyst-vegetative cell septa than in the septa between
204 vegetative cells explains why we could readily observe the difference by electron
205 microcopy only in the former.

206 We also looked at the morphology of filaments incubated for 48 h in $BG11_0$
207 medium by labeling the cytoplasmic membrane with the FM 1-43 fluorescent probe
208 (Schneider *et al.*, 2007; Nürnberg *et al.*, 2014). The stain marked the periphery of the
209 heterocysts as well as that of vegetative cells (Fig. 4B). As seen with this label, the
210 heterocyst necks were clearly wider in WT+pSepJ than in the wild type, corroborating
211 the observations made by electron microcopy and staining with Van-FL.

212

213 *Localization of SepJ-GFP in a SepJ overproducing strain*

214 Strain CSDN11 bears in its chromosome a construct in which a *sepJ-gfp* fusion gene is
215 expressed from the native *sepJ* promoter and a wild-type *sepJ* gene is expressed from
216 the C.K3 cassette (Fig. 6A), which promotes high expression of downstream genes
217 (Frías *et al.*, 2000). We used as a control strain CSAM137, which only bears *sepJ-gfp*
218 expressed from the native *sepJ* promoter (Flores *et al.*, 2007). GFP fluorescence in
219 strain CSDN11 (*sepJ-gfp*, C.K3-*sepJ*) was observed at the intercellular septa (Fig. 6B),
220 as is normally the case for SepJ-GFP. However, whereas wild-type expression in strain

CSAM137 (*sepJ-gfp*) results in SepJ-GFP spots that are focused in the center of the septa (Fig. 6C; Flores *et al.*, 2007), in strain CSDN11 (*sepJ-gfp*, C.K3-*sepJ*) the GFP signal was frequently observed spread along the septa (Fig. 6B). For comparison of SepJ-GFP distribution in the two strains, the fluorescence intensity was plotted against the position in the septum, a Gaussian model was fitted to the data, and the full width at half maximum (FWHM) was determined (Fig. 6D). However, when light travels through the lens system of a microscope it is diffracted and thus changes the size of an object, letting it appear much bigger than its actual size. To correct for the point spread, we used labeling with FM 1-43, which highlights the cytoplasmic membrane and thus defines a distance of approximately 4 nm (Mitra *et al.*, 2004). The corrected FWHM value (see Experimental procedures) was 1.00 ± 0.23 µm for CSDN11 and 0.43 ± 0.10 µm for CSAM137. Hence, SepJ was around two times more widely distributed in CSDN11 than in CSAM137, indicating that over-expression of SepJ induces a wide distribution of SepJ-GFP.

Intercellular junctions and communication

Because of the wide heterocyst-vegetative cell septa present in WT+pSepJ, we investigated structures and functions related to intercellular communication. Murein sacculi corresponding to several cell units have been previously isolated from the heterocyst-forming cyanobacteria *Anabaena cylindrica* (Dunn and Wolk, 1970), *Nostoc punctiforme* (Lehner *et al.*, 2011) and *Anabaena* (Nürnberg *et al.*, 2015). Here we isolated sacculi of up to about eleven cells from *Anabaena* (Fig. 7A). In some sacculi, dense circular areas likely corresponding to juxtaposed peptidoglycan from adjacent cells (septal peptidoglycan disks) could be observed (Fig. 7B). As previously reported (Lehner *et al.*, 2013; Nürnberg *et al.*, 2015; Rudolf *et al.*, 2015), a number of nanopores

could be observed in these disks (Fig. 7C). The number of nanopores in the peptidoglycan disks from septa between vegetative cells was quantified. In filaments grown in $BG11_0$ medium, we observed a 1.4-fold increase in the number of nanopores in the SepJ-overexpressing strain as compared to the wild type (WT+pSepJ, 68.3 ± 4.3 nanopores/disk [mean ± SEM], n = 6 disks counted; *Anabaena*, 48.75 ± 3.8 nanopores/disk, n = 4; Student's *t* test $p = 0.007$). In filaments grown in BG11 medium, a 1.38-fold increase was observed (WT+pSepJ, 71.9 ± 9.7 nanopores/disk, n = 8; wild type, 52.3 ± 6.2 nanopores/disk, n = 9; $p = 0.024$). Additionally, these perforations were more spread in WT+pSepJ than in the wild type, in which the nanopores were located in a relatively small area in the central part of the disk (Fig. 7C), as previously noted (Lehner *et al.*, 2013). We were not able, however, to establish a difference between the two strains in the diameter of the nanopores.

As described earlier, intercellular transfer of some fluorescent tracers is altered in *Anabaena* mutants of the septal proteins. We therefore tested intercellular transfer of calcein and 5-CF in WT+pSepJ and, for comparison, the wild type. Fluorescence recovery after photobleaching (FRAP) analysis was performed as described in Experimental procedures and the results are presented as the recovery constant, *R*. As shown in Table 1, transfer of neither calcein nor 5-CF was different between the two strains for vegetative cells in nitrate-grown filaments or in filaments that had been incubated in the absence of combined nitrogen for 48 h. In contrast, when transfer from vegetative cells to heterocysts was tested, it was found that transfer of calcein was 1.73-fold higher in WT+pSepJ than in the wild type, a significant difference. Nonetheless, transfer of 5-CF to heterocysts was similar in both strains. These results indicate that increased expression of SepJ increases rates of intercellular molecular exchange

noticeably between vegetative cells and heterocysts, but this increase is selective and does not apply to all molecules tested.

Heterocyst pattern

When WT+pSepJ was incubated in $BG11_0$ medium, it showed altered heterocyst frequency and distribution in the filament. Heterocyst frequency was lower in WT+pSepJ than in the wild type at both 24 and 48 h after N step-down, although the percentage of contiguous heterocysts, which were observed as heterocyst doublets, was higher in the mutant (Table 2). The mean interval of cells between heterocysts was larger in strain WT+pSepJ than in the wild type at 24 h, but somewhat smaller at 48 h (see Fig. 8 and Table 2). Thus, overexpression of SepJ altered regulation of heterocyst differentiation affecting heterocyst pattern.

To test possible epistastic relations between SepJ, PatS and HetN, we transferred pCSAM200::C.K1-*sepJ* to mutants bearing deletions in *patS* (strain CSVT20), producing strain CSVM20 (Δ*patS*+pSepJ), and *hetN* (strain CSL7), producing strain CSVM21 (Δ*hetN*+pSepJ). Western blot analysis showed the presence of higher levels of SepJ in Δ*patS*+pSepJ and Δ*hetN*+pSepJ than in their respective parental strains (Fig. 1C).

Strain CSVT20 (Δ*patS*) produces more heterocysts (including contiguous heterocysts) and shorter intervals of vegetative cells between heterocysts than the wild type (Corrales-Guerrero *et al.*, 2013). In Δ*patS*+pSepJ, heterocyst frequency was similar to that in Δ*patS* at both 24 and 48 h after N step-down (Table 2; Fig. 8). Thus, in contrast to what happened in the wild-type background, in which overexpression of SepJ resulted in a decrease in heterocyst frequency, in the *patS* background such

alteration was not observed. Nonetheless, the percentage of heterocyst doublets was higher in Δ*patS*+pSepJ than in Δ*patS*, and this effect was larger at 48 h than at 24 h. Mean interval size was significantly ($p < 0.05$) lower in Δ*patS*+pSepJ than in Δ*patS* only at 48 h. Thus, the heterocyst pattern was affected by overexpression of SepJ.

Strain CSL7 (Δ*hetN*) also produces more heterocysts (including contiguous heterocysts) and shorter intervals of vegetative cells between heterocysts than the wild type (Corrales-Guerrero *et al.*, 2014a). In Δ*hetN*+pSepJ, heterocyst frequency was decreased, whereas the percentage of heterocyst doublets and the mean interval size were increased, with regard to strain CSL7 at 24 h after N step-down (Table 2; Fig. 8). However, no statistically significant differences were observed at 48 h between Δ*hetN*+pSepJ and Δ*hetN* (Table 2). SepJ overexpression in the *hetN* background resulted in a deficit in the diazotrophic growth of strain Δ*hetN*+pSepJ on solid medium similar to that of strain WT+pSepJ (Fig. 2).

Discussion

Here we have shown that overexpression of *sepJ* in *Anabaena* results in a distribution of a SepJ-GFP fusion protein in the intercellular septa that is wider than that observed when SepJ-GFP is the only SepJ form present in the cells (Flores *et al.*, 2007; Mariscal *et al.*, 2011). This observation indicates a wide distribution of the combined population of SepJ-GFP and SepJ in the intercellular septa of the SepJ overproducing strain. A wide distribution of SepJ in the septa has also been observed by immunogold labeling in an independently isolated *sepJ* overexpressing strain (Omairi-Nasser *et al.*, 2015), but this strain was not further characterized. Our SepJ-overexpressing strain, WT+pSepJ, additionally makes intercellular septa that are wider than those observed in the wild

type. The increased size can be noticed in septa between vegetative cells (Fig. 5), but is striking in the septa between heterocysts and vegetative cells (Figs. 3 and 4). It appears that the wide distribution of SepJ resulting from the increased expression of *sepJ* alters cellular structure making the septa wider than in the wild type, and that during heterocyst differentiation this results in septa that cannot be restricted in size. The heterocysts present in WT+SepJ support only low nitrogenase activity resulting in impaired diazotrophic growth. This low nitrogenase activity might result from the low percentage of heterocysts, from the presence of contiguous heterocysts that may not receive enough reductant from vegetative cells, and from an increased exposure to oxygen through the enlarged vegetative cell-heterocyst septa. According to Walsby (2007), the reduction in the area of cell-cell connection between vegetative cells and heterocysts is required to diminish the entry of O_2 into the heterocysts and allow functionality of the oxygen-sensitive nitrogenase. However, we observed only a 2-fold increase in nitrogenase activity under anoxic conditions in WT+pSepJ, similar to the increase found in the wild type.

As described in the Introduction, nanopores have been visualized in septal peptidoglycan disks from different heterocyst-forming cyanobacteria. An AmiC-type cell wall amidase has been suggested to have a role in drilling holes into the septal cross-walls (Lehner et al., 2013). Whereas the decreased number of nanopores observed in mutants lacking SepJ or/and FraC/FraD implies that formation of those structures requires the presence of these proteins (Nürnberg *et al.*, 2015), the increased number of nanopores observed in the SepJ-overexpressing strain corroborates involvement of SepJ. Consistent with the spread location of the SepJ-GFP signal at the intercellular septa of a *sepJ* overexpressing strain (Fig. 6), the nanopores are very spread out in the

342 septal peptidoglycan disk of the SepJ-overproducing strain (Fig. 7). Thus, SepJ could be
343 a primer promoting nanopore formation by septal AmiC-type amidases.

344 We have previously suggested the presence in *Anabaena* of two types of septal
345 junction complexes, one related to SepJ with preference for calcein and another related
346 to FraCD with preference for 5-CF (Merino-Puerto *et al.*, 2011; Nürnberg *et al.*, 2015).
347 Calcein is larger and more negatively charged than 5-CF (Nürnberg *et al.*, 2015). The
348 SepJ-overexpressing strain exhibits an increased intercellular transfer of calcein
349 between vegetative cells and heterocysts, whereas transfer between vegetative cells is
350 not apparently affected (Table 1). Interestingly, transfer of 5-CF is not significantly
351 affected in any case. This implies that SepJ-related septal junctions do not limit calcein
352 or 5-CF transfer between vegetative cells, whereas transfer of calcein between
353 vegetative cells and heterocysts appears limited in the wild type so that it is increased by
354 increasing SepJ levels. This is consistent with the fact that calcein transfer is higher
355 between vegetative cells than between vegetative cells and heterocysts in *Anabaena*
356 (Mullineaux *et al.*, 2008). The effect of SepJ overexpression specifically on calcein
357 transfer is also consistent with the idea that the SepJ-related septal junction complexes
358 have some preference for calcein. Because *sepJ* inactivation mutants do not produce
359 mature heterocysts, a role of SepJ in calcein transfer between vegetative cells and
360 heterocysts could not be studied before. Thus, this is the first report showing that SepJ
361 is involved in the molecular exchange between vegetative cells and heterocysts that can
362 be probed with calcein.

363 Overexpression of SepJ also alters heterocyst pattern and leads to a lower level
364 of heterocyst differentiation in WT+pSepJ than in the wild type. Because the
365 intercellular transfer of PatS- (Corrales-Guerrero *et al.*, 2015) or HetN-dependent
366 (Rivers *et al.*, 2014) regulators has been associated with SepJ, we performed epistasis

analysis by testing the effect of overexpression of SepJ in Δ*patS* or Δ*hetN* genetic backgrounds. The inhibitory effect of SepJ overexpression on the production of heterocysts is not observed in the Δ*patS* mutant, implying that PatS is needed for this effect to be manifest. Additionally, overexpression of SepJ in the Δ*hetN* background is accompanied by a decrease in the percentage of heterocysts and an increase in the mean interval size and percentage of heterocyst doublets that was only observed 24 h after N step-down. These observations are consistent with a role of SepJ in the intercellular transfer of the inhibitory PatS morphogen. On the other hand, the decreased mean interval size and increased percentage of heterocyst doublets observed in Δ*patS*+pSepJ as compared to Δ*patS*, which were larger at 48 h than at 24 h, imply a role of SepJ in the transfer of a factor other than PatS influencing heterocyst pattern. This factor could be a HetN-dependent regulatory signal (Rivers *et al*., 2014), which is thought to act later than PatS (Callahan and Buikema, 2001). Consistently, no effects of overexpression of SepJ are observed in the Δ*hetN* background at 48 h after N step-down. Taken together, the results of our epistasis analysis imply a role of SepJ in the intercellular transfer of the PatS morphogen and, possibly, of the HetN-dependent regulatory signal.

Overexpression of SepJ resulted in an increased frequency of heterocyst doublets in the different genetic backgrounds tested, except in Δ*hetN*+pSepJ at 48 h. This implies a decreased accumulation of the inhibitory signals in the cells contiguous to (pro)heterocysts, which could result from increased transfer among vegetative cells. The increased transfer of calcein specifically between vegetative cells and heterocysts in the SepJ overexpression strain discussed above might be taken to imply that the step of transfer of regulatory signals from the heterocyst to its neighboring vegetative cells is also stimulated by overexpression of SepJ. However, the possibility remains that, in the wild type, the amount of SepJ limits the transfer of calcein between vegetative cells and

heterocysts but not of the heterocyst regulators between (pro)heterocysts and vegetative cells. In this case, the effect of SepJ overexpression on the heterocyst pattern could result only from an increased transfer of the regulators between vegetative cells.

Epistasis analysis similar to that done here for *sepJ* and *patS* or *hetN* has been recently performed for *hetC* and *patS* or *hetN*. The results of these analyses are consistent with the idea that the HetC ABC exporter participates in export from proheterocysts of the PatS morphogen (Corrales-Guerrero *et al.*, 2014b) or of the PatS morphogen and a HetN-dependent signal (Videau *et al.*, 2015). The existence of a transporter specific for export of the regulators from the (pro)heterocysts to their neighboring vegetative cells could make transfer not limited to a SepJ-dependent pathway. Nonetheless, if SepJ participates in the transfer of regulators from the (pro)heterocysts, the activity of a transporter such as HetC could be combined with transfer through SepJ-related septal junctions. Interestingly, a HetC-GFP fusion protein shows a preferential localization at the heterocyst poles (the region known as heterocyst neck), where a SepJ-GFP fusion is also located (Flores *et al.*, 2007; Flores and Herrero, 2010; Omairi-Nasser *et al.*, 2015).

Based on expression of a P_{hetR}-*gfp* transcriptional fusion in a *sepJ* (*fraG*) background, it has been suggested that SepJ is not needed for proper heterocyst pattern formation (Nayar *et al.*, 2007). However, the results described in this work and those of other recent studies (Corrales-Guerrero *et al.*, 2014b, 2015; Videau *et al.*, 2015) have unraveled possible relations between SepJ and PatS and HetN, as well as between HetC and PatS and HetN, affecting heterocyst pattern formation. Heterocyst differentiation aborts early in *sepJ* (Flores *et al.*, 2007; Nayar *et al.*, 2007) and *hetC* (Khudyakov and Wolk, 1997; Xu and Wolk, 2001) inactivation mutants, an effect that could result from accumulation of inhibitory PatS that is not exported from proheterocysts.

Experimental procedures

Strains and growth conditions

Anabaena sp. strain PCC 7120 and derived strains were grown in BG11 (containing $NaNO_3$) or $BG11_0$ (lacking nitrate) medium at 30 ºC in the light (25 μE m^{-2} s^{-1} from fluorescent lamps), in shaken (100 r.p.m.) liquid cultures or in medium solidified with 1 % (w/v) Difco agar. Antibiotics were used at the following concentrations: Sm, 5 μg ml^{-1}; Sp, 5 μg ml^{-1} and Nm, 50 μg ml^{-1}. Heterocyst formation was induced by growth in $BG11_0$ medium. For transfer between media, cells were harvested by centrifugation (3,000 x g) and washed three times with the appropriate medium.

Escherichia coli DH5α was used for plasmid constructions, and strains HB101 and ED8654 for conjugations with *Anabaena* strains. They were grown in LB medium, supplemented when appropriate with antibiotics at standard concentrations (Ausubel *et al*., 2014).

Construction of mutants

The genomic sequence of *Anabaena* is available (Kaneko *et al.*, 2001). For construction of pCSDN2a and pCSDN2b, genomic DNA from *Anabaena* was amplified by PCR with primers Alr2338-7 (chromosome coordinates 2818355 - 2818375) and Alr2338-10 (chromosome coordinates: 2820781 - 2820764) and cloned in plasmid pMBL-T (Canvax) producing pCSVM58. After verification by sequencing that the amplification product did not contain mutations, the C.K1 resistance cassette (obtained from pRL161 digested with BamHI and filled with Klenow enzyme) was inserted into SmaI-ended pCSVM58 plasmid, and clones bearing the two possible orientations of C.K1 with

441 respect to *sepJ* were selected. pCSVM59a bears C.K1 in the same orientation as *sepJ*,
442 and pCSVM59b bears C.K1 in opposite orientation. C.K1-*sepJ* was extracted from
443 plasmids pCSVM58a and pCSVM58b and inserted into the self-replicating vector
444 pCSAM200 (Ionescu *et al.*, 2010) using EcoRI restriction sites, producing pCSDN2a
445 and pCSDN2b, respectively. Cassette C.K1 bears the *npt* gene and its own natural
446 promoter (Elhai and Wolk, 1988).

447 Plasmid pCSDN11 was generated by amplifying *sepJ-gfp* from genomic DNA
448 of strain CSAM137 (Flores *et al*., 2007) using primers Alr2338-7 and pRL500-1 (5'-
449 ATAGGCGTATCACGAGGC-3') and inserting the fragment into pSpark (Canvax).
450 Correctness of the inserted sequence was verified by sequencing. The resulting plasmid
451 was digested with SalI and the fragment was inserted into XhoI-digested plasmid
452 pRL278, which cannot replicate in *Anabaena* (Black *et al*., 1993).

453 Plasmids were transferred to *Anabaena* strains by conjugation as previously
454 described (Elhai *et al.,* 1997). pCSDN2a was transferred to *Anabaena* wild type and
455 strains CSVT20 (Δ*patS*) and CSL7 (Δ*hetN*) with selection for resistance to Sm and Sp
456 producing strains CSDN2a, CSVM20 and CSVM21, respectively. pCSDN2b was
457 transferred to *Anabaena* with selection for resistance to Sm and Sp producing strain
458 CSDN2b. Strain CSDN11 was generated by transferring pCSDN11 to *Anabaena* with
459 selection for resistance to Nm.

460

461 *Labeling with dyes*

462 Staining with vancomycin-FL (Van-FL) was used to visualize septa between cells
463 (Lehner *et al*., 2013), and was performed in filaments grown in BG11 medium or
464 incubated for 24 or 48 hours in $BG11_0$ medium as previously reported (Nürnberg *et al*.,

2015). Staining was performed mixing 0.1 ml of a filament suspension with 2 µl of a stock solution containing 100 µg Van-FL/ml dimethyl sulfoxide (DMSO) (Van-FL was purchased from Invitrogen).

Staining with FM 1-43 was used to visualize the inner and outer cytoplasmic membrane of cyanobacteria (Schneider *et al.*, 2007). For labeling, 2.5 µl FM 1-43 (0.1 mg/ml DMSO; Molecular Probes) was added to 0.1 ml of culture. The suspension was incubated for 10 min at room temperature and washed twice with growth medium prior visualization.

Alcian Blue was used to visualize the polysaccharide layer of (pro)heterocysts (Corrales-Guerrero *et al.*, 2014). For staining, cell suspensions were mixed (1:2) with a filtered 1 % (w/v) Alcian blue (Sigma) solution in water and visualized under standard light microscopy.

Growth rates

The growth rate constant ($\mu=[\ln 2]/t_d$, where t_d is the doubling time) was calculated from the increase in $OD_{750\ nm}$ of shaken liquid cultures. Cultures were inoculated with an amount of cells giving an $OD_{750\ nm}$ of about 0.05 (light path, 1 cm) and grew logarithmically until reaching an $OD_{750\ nm}$ of about 0.8-0.9. The suspensions of filaments were carefully homogenized with a pipette before taking the samples.

Standard, confocal and fluorescence microscopy

For standard light microscopy, filaments grown in BG11 medium (in the presence of Sm and Sp for the mutants) were harvested, washed three times with nitrogen-free ($BG11_0$) medium and resuspended in the same medium without antibiotics. After 24 h

of incubation at 30ºC in the light, samples were visualized by standard light microscopy. For cell counting, dividing cells were counted as two cells.

For confocal microscopy, samples were visualized using a 63X 1.4 NA oil immersion objective attached to a Leica TCS SP2 or Leica SP5 confocal laser-scanning microscope. GFP was excited using 488-nm irradiation from an argon ion laser. Fluorescent emission was monitored by collection across windows of 500-540 nm (GFP imaging) and 630-700 nm or 670-720 nm (cyanobacterial autofluorescence).

For fluorescence microscopy, samples were visualized in a Leica DM6000B fluorescence microscope with an ORCA-ER camera (Hamamatsu). Fluorescence was monitored using a FITC L5 filter (excitation, band-pass [BP] 480/40 filter; emission, BP 527/30 filter). Images were treated with the Leica Application Suite Advanced Fluorescence software and merged with ImageJ 1.47i software (http://imagej.nih.gov/ij).

To correct for the point spread in the analysis of SepJ-GFP (Fig. 6), images were taken with the same settings using *Anabaena* cells stained with FM 1-43. The full width at half maximum (FWHM) fluorescence was determined in 36 septa and the corrected FWHM of SepJ fluorescence was calculated using the formula $FWHM' = (FWHM^2 - PSF^2)^{-0.5}$, where FWHM is the initially observed FWHM of the SepJ fluorescence and PSF is the FWHM of the FM 1-43 fluorescence.

Electron microscopy

Filaments incubated in $BG11_0$ for 24 h were harvested by gentle centrifugation and fixed with 2.5 % (w/v) glutaraldehyde and 1 % (w/v) OsO_4, dehydrated with increasing

concentrations of acetone, embedded in Spurr resin, and ultra-thin sections were prepared and post-stained with 2 % (w/v) uranyl acetate. The sacculi were isolated and analyzed as described previously (Lehner *et al*., 2013; Nurnberg *et al*., 2015). The purified sacculi were deposited on formvar/carbon film coated copper grids, and stained with 1% (w/v) uranyl acetate. All the samples were examined with a ZEISS LIBRA 120 PLUS electron microscope at 120 kV.

Intercellular transfer of calcein and 5-CF

For calcein and 5-CF transfer assays, calcein and 5-CF staining and FRAP analysis were performed as previously reported (Mullineaux *et al*., 2008; Merino-Puerto *et al*., 2011; Nürnberg et al., 2014). Cell suspensions were spotted onto BG11 or $BG11_0$ agar and placed in a custom-built temperature-controlled sample holder with a glass cover slip on top. All measurements were carried out at 30°C. For both calcein and 5-CF, cells were imaged with a Leica TCS SP5 confocal laser-scanning microscope using a x63 oil-immersion objective (NA 1.4) and a 488 nm line argon laser as the excitation source. Fluorescence emission was monitored by collection across windows of 500-527 nm. A maximally opened pinhole of 600 µm, corresponding to an optical section thickness of 4.2 µm was used. After an initial image was recorded (pre-bleach), the bleach was carried out by increasing the laser intensity and zooming into the region of interest, and the recovery was recorded.

Acknowledgements

Work in Seville was supported by grant BFU2014-56757-P from Plan Nacional de Investigación, Spain, co-financed by the European Regional Development Fund. DJN was supported by a Queen Mary University of London College Studentship and the University of London Central Research Fund.

Conflict of interest

The authors declare that they have no conflict of interest.

Author Contributions

All authors designed research, interpreted data and corrected the manuscript; VM and DJN constructed mutants and acquired and analyzed data; EF wrote the manuscript.

References

Ausubel, F.M., Brent, R., Kingston, R.E., Moore, D.D., Seidman, J.G., Smith, J.A., and Struhl, K. (2014) Current Protocols in Molecular Biology. New York: *Greene Publishing and Wiley-Interscience.*

Black, T.A., Cai, Y., and Wolk, C.P. (1993) Spatial expression and autoregulation of *hetR*, a gene involved in the control of heterocyst development in *Anabaena*. *Mol Microbiol* **9:** 77-84.

Burnat, M., Schleiff, E., and Flores, E. (2014) Cell envelope components influencing filament length in the heterocyst-forming cyanobacterium *Anabaena* sp. strain PCC 7120. *J Bacteriol* **196:** 4026-4035.

Callahan, S.M., and Buikema, W.J. (2001) The role of HetN in maintenance of the heterocyst pattern in *Anabaena* sp. PCC 7120. *Mol Microbiol* **40:** 941-950.

Corrales-Guerrero, L., Mariscal, V., Flores, E., and Herrero, A. (2013) Functional dissection and evidence for intercellular transfer of the heterocyst-differentiation PatS morphogen. *Mol Microbiol* **88:** 1093-1105.

Corrales-Guerrero, L., Mariscal, V., Nürnberg, D.J., Elhai, J., Mullineaux, C.W., Flores, E., and Herrero, A. (2014a) Subcellular localization and clues for the function of the HetN factor influencing heterocyst distribution in *Anabaena* sp. strain PCC 7120. *J Bacteriol* **196:** 3452-3460.

Corrales-Guerrero, L., Flores, E., and Herrero, A. (2014b) Relationships between the ABC-exporter HetC and peptides that regulate the spatiotemporal pattern of heterocyst distribution in *Anabaena*. *PLoS One* **9:** e104571.

Corrales-Guerrero, L., Tal, A., Arbel-Goren, R., Mariscal, V., Flores, E., Herrero, A., and Stavans, J. (2015) Spatial fluctuations in expression of the heterocyst differentiation regulatory gene *hetR* in *Anabaena* filaments. *PLoS Genet* **11:** e1005031.

Daniel RA, and Errington J. (2003) Control of cell morphogenesis in bacteria: two distinct ways to make a rod-shaped cell. *Cell* **113:** 767-776.

Dunn, J.H., and Wolk, C.P. (1970) Composition of the cellular envelopes of *Anabaena cylindrica*. *J Bacteriol* **103:** 153-8.

Elhai, J., and Wolk, C.P. (1988) A versatile class of positive-selection vectors based on the nonviability of palindrome-containing plasmids that allows cloning into long polylinkers. *Gene* **68:** 119-138.

Elhai, J., Vepritskiy, A., Muro-Pastor, A.M., Flores, E., and Wolk, C.P. (1997) Reduction of conjugal transfer efficiency by three restriction activities of *Anabaena* sp. strain PCC 7120. *J Bacteriol* **179:** 1998-2005.

Feldmann EA, Ni S, Sahu ID, Mishler CH, Risser DD, Murakami JL, Tom SK, McCarrick, RM, Lorigan, GA, Tolbert BS, Callahan SM, Kennedy MA (2011) Evidence for direct binding between HetR from *Anabaena* sp. PCC 7120 and PatS-5. *Biochemistry* **50:** 9212-9224.

Feldmann, E.A., Ni, S., Sahu, I.D., Mishler, C.H., Levengood, J.D., Kushnir, Y., McCarrick, R.M., Lorigan, G.A., Tolbert, B.S., Callahan, S.M., and Kennedy, M.A. (2012) Differential binding between PatS C-terminal peptide fragments and HetR from *Anabaena* sp. PCC 7120. *Biochemistry* 51:2436-2442.

Flores, E., and Herrero, A. (2010) Compartmentalized function through cell differentiation in filamentous cyanobacteria. *Nat Rev Microbiol* **8:** 39-50.

Flores, E., Pernil, R., Muro-Pastor, A.M., Mariscal, V., Maldener, I., Lechno-Yossef, S., Fan, Q., Wolk, C.P., and Herrero, A. (2007) Septum-localized protein required for filament integrity and diazotrophy in the heterocyst-forming cyanobacterium *Anabaena* sp. strain PCC 7120. *J Bacteriol* **189:** 3884-3890.

Flores, E., Herrero, A., Forchhammer, K., and Maldener, I. (2016) Septal junctions in filamentous heterocyst-forming cyanobacteria. *Trends Microbiol* **24:** 79-82.

Frías, J.E., Flores, E., and Herrero, A. (2000) Activation of the *Anabaena nir* operon promoter requires both NtcA (CAP family) and NtcB (LysR family) transcription factors. *Mol Microbiol* **38:** 613-625.

593 Giddings, T.H., and Staehelin, L.A. (1978) Plasma membrane architecture of *Anabaena cylindrica*:
594 occurrence of microplasmodesmata and changes associated with heterocyst development and the cell
595 cycle. *Cytobiologie* **16:** 235-249.

596 Giddings, T.H., and Staehelin, L.A. (1981) Observation of microplasmodesmata in both heterocyst-
597 forming and non-heterocyst forming filamentous cyanobacteria by freeze-fracture electron microscopy.
598 *Arch Microbiol* **129:** 295-298.

599 Hahn, A., and Schleiff, E. (2014) The cell envelope. In *The Cell Biology of Cyanobacteria*. Flores, E. and
600 Herrero, A. (eds.). Norfolk, UK: Caister Academic Press. pp. 29-87.

601 Herrero, A., Picossi, S., and Flores, E. (2013) Gene expression during heterocyst differentiation. *Adv Bot*
602 *Research* **65:** 281-329.

603 Higa, K.C., Rajagopalan, R., Risser, D.D., Rivers, O.S., Tom, S.K., Videau, P., and Callahan, S.M.
604 (2012) The RGSGR amino acid motif of the intercellular signaling protein, HetN, is required for
605 patterning of heterocysts in *Anabaena* sp. strain PCC 7120. *Mol Microbiol* **83:** 682-693.

606 Huang X, Dong Y, Zhao J (2004) HetR homodimer is a DNA-binding protein required for heterocyst
607 differentiation, and the DNA-binding activity is inhibited by PatS. *Proc Natl Acad Sci USA* **101:** 4848-
608 4853.

609 Ionescu, D., Voss, B., Oren, A., Hess, W.R., and Muro-Pastor, A.M. (2010) Heterocyst-specific
610 transcription of NsiR1, a non-coding RNA encoded in a tandem array of direct repeats in cyanobacteria. *J*
611 *Mol Biol* **398:** 177–188.

612 Kaneko, T., Nakamura, Y., Wolk, C.P., Kuritz, T., Sasamoto, S., Watanabe, A., Iriguchi, M., Ishikawa,
613 A., Kawashima, K., Kimura, T., Kishida, Y., Kohara, M., Matsumoto, M., Matsuno, A., Muraki, A.,
614 Nakazaki, N., Shimpo, S., Sugimoto, M., Takazawa, M., Yamada, M., Yasuda, M., and Tabata, S. (2001)
615 Complete genomic sequence of the filamentous nitrogen-fixing cyanobacterium *Anabaena* sp. strain PCC
616 7120. *DNA Res* **8:** 205-213.

617 Khudyakov, I.Y., and Golden, J.W. (2004) Different functions of HetR, a master regulator of heterocyst
618 differentiation in *Anabaena* sp. PCC 7120, can be separated by mutation. *Proc Natl Acad Sci U S A* **101:**
619 16040-16045.

620 Khudyakov, I., and Wolk, C.P. (1997) *hetC*, a gene coding for a protein similar to bacterial ABC protein
621 exporters, is involved in early regulation of heterocyst differentiation in *Anabaena* sp. strain PCC 7120. *J*
622 *Bacteriol* **179:** 6971-6978.

623 Kumar, K., Mella-Herrera, R.A., Golden, and J.W. (2010) Cyanobacterial heterocysts. *Cold Spring Harb*
624 *Perspect Biol* **2:** a000315.

625 Lang, N.J., and Fay, P. (1971) The heterocysts of blue-green algae. II. Details of ultrastructure. *Proc R*
626 *Soc Lond B* **178:** 193-203.

627 Lehner, J., Zhang, Y., Berendt, S., Rasse, T.M., Forchhammer, K., and Maldener, I. (2011) The
628 morphogene AmiC2 is pivotal for multicellular development in the cyanobacterium *Nostoc* punctiforme.
629 *Mol Microbiol* **79:** 1655-1669.

630 Lehner, J., Berendt, S., Dörsam, B., Pérez, R., Forchhammer, K., and Maldener, I. (2013) Prokaryotic
631 multicellularity: a nanopore array for bacterial cell communication. *FASEB J* **27:** 2293-30.

632 Mariscal, V. (2014) Cell-cell joining proteins in heterocyst-forming cyanobacteria. In *The Cell Biology of*
633 *Cyanobacteria*. Flores, E. and Herrero, A. (eds.). Norfolk, UK: Caister Academic Press. pp. 293-304.

634 Mariscal, V., Herrero, A., Nenninger, A., Mullineaux, C.W., and Flores, E. (2011) Functional dissection
635 of the three-domain SepJ protein joining the cells in cyanobacterial trichomes. *Mol Microbiol* **79:** 1077-
636 1088.

Merino-Puerto, V., Mariscal, V., Mullineaux, C.W., Herrero, A., and Flores, E. (2010) Fra proteins influencing filament integrity, diazotrophy and localization of septal protein SepJ in the heterocyst-forming cyanobacterium *Anabaena* sp. *Mol Microbiol* **75:** 1159-1170.

Merino-Puerto, V., Schwarz, H., Maldener, I., Mariscal, V., Mullineaux, C.W., Herrero, A., and Flores, E. (2011) FraC/FraD-dependent intercellular molecular exchange in the filaments of a heterocyst-forming cyanobacterium, *Anabaena* sp. *Mol Microbiol* **82:** 87-98.

Mitra, K., Ubarretxena-Belandia, I., Taguchi, T., Warren, G. and Engelman, D.M. (2004) Modulation of the bilayer thickness of exocytic pathway membranes by membrane proteins rather than cholesterol. *Proc Natl Acad Sci USA* **101:** 4083-4088.

Mullineaux, C.W., and Nürnberg, D.J. (2014) Tracing the path of a prokaryotic paracrine signal. *Mol Microbiol* **94:** 1208-1212.

Mullineaux, C.W., Mariscal, V., Nenninger, A., Khanum, H., Herrero, A., Flores, E., and Adams, D.G. (2008) Mechanism of intercellular molecular exchange in heterocyst-forming cyanobacteria. *EMBO J* **27:** 1299-1308.

Nayar, A.S., Yamaura, H., Rajagopalan, R., Risser, D.D., and Callahan, S.M. (2007) FraG is necessary for filament integrity and heterocyst maturation in the cyanobacterium *Anabaena* sp. strain PCC 7120. *Microbiology* **153:** 601-603.

Nürnberg, D.J., Mariscal, V., Parker, J., Mastroianni, G., Flores, E., and Mullineaux, C.W. (2014) Branching and intercellular communication in the Section V cyanobacterium *Mastigocladus laminosus*, a complex multicellular prokaryote. *Mol Microbiol* **91:** 935-949.

Nürnberg, D.J., Mariscal, V., Bornikoel, J., Nieves-Morión, M., Krauß, N., Herrero, A., Maldener, I., Flores, E., and Mullineaux, C.W. (2015) Intercellular diffusion of a fluorescent sucrose analog via the septal junctions in a filamentous cyanobacterium. *mBio* **6(2):** e02109.

Omairi-Nasser, A., Haselkorn, R., and Austin II, J. (2014) Visualization of channels connecting cells in filamentous nitrogen-fixing cyanobacteria. *FASEB J* **28:** 3016-3022.

Omairi-Nasser, A., Mariscal, V., Austin, J.R., and Haselkorn, R. (2015) Requirement of Fra proteins for communication channels between cells in the filamentous nitrogen-fixing cyanobacterium *Anabaena* sp. PCC 7120. *Proc Natl Acad Sci USA* **112**: E4458-4464.

Risser DD, Callahan SM (2009) Genetic and cytological evidence that heterocyst patterning is regulated by inhibitor gradients that promote activator decay. *Proc Natl Acad Sci USA* **106:** 19884-19888.

Rivers, O.S., Videau, P., and Callahan, S.M. (2014) Mutation of *sepJ* reduces the intercellular signal range of a *hetN*-dependent paracrine signal, but not of a *patS*-dependent signal, in the filamentous cyanobacterium *Anabaena* sp. strain PCC 7120. *Mol Microbiol* **94:** 1260-1271.

Rudolf, M., Tetik, N., Ramos-León, F., Flinner, N., Ngo, G., Stevanovic, M., Burnat, M., Pernil, R., Flores, E., and Schleiff, E. (2015) The peptidoglycan-binding protein SjcF1 influences septal junction function and channel formation in the filamentous cyanobacterium *Anabaena*. *mBio* **6(4):** e00376-15.

Schneider, D., Fuhrmann, E., Scholz, I., Hess, W.R., and Graumann, P.L. (2007) Fluorescence staining of live cyanobacterial cells suggest non-stringent chromosome segregation and absence of a connection between cytoplasmic and thylakoid membranes. *BMC Cell Biol* **8:** 39.

Tiyanont, K., Doan, T., Lazarus, M.B., Fang, X., Rudner, D.Z., and Walker, S. (2006) Imaging peptidoglycan biosynthesis in *Bacillus subtilis* with fluorescence antibiotics. *Proc Natl Acad Sci USA* **103:**11033-11038.

Valladares, A., Flores, E., and Herrero, A. (2016) The heterocyst differentiation transcriptional regulator HetR of the filamentous cyanobacterium *Anabaena* forms tetramers and can be regulated by phosphorylation. *Mol Microbiol* **99:** 808-819.

682 Vázquez-Bermúdez, M.F., Herrero, A., and Flores, E. (2000) Uptake of 2-oxoglutarate in *Synechococcus*
683 strains transformed with the *Escherichia coli kgtP* gene. *J Bacteriol* **182:** 211-215.

684 Videau, P., Rivers, O.S., Higa, K.C., and Callahan, S.M. (2015) ABC transporter required for
685 intercellular transfer of developmental signals in a heterocystous cyanobacterium. *J Bacteriol* **197:** 2685-
686 2693.

687 Walsby, A.E. (2007) Cyanobacterial heterocysts: terminal pores proposed as sites of gas exchange.
688 *Trends Microbiol* **15**: 340–349.

689 Wilcox, M., Mitchison, G.J., and Smith, R.J. (1973) Pattern formation in the blue-green alga, *Anabaena*.
690 *J Cell Sci* **12:** 707–723.

691 Wilk, L., Strauss, M., Rudolf, M., Nicolaisen, K., Flores, E., Kühlbrandt, W., and Schleiff, E. (2011)
692 Outer membrane continuity and septosome formation between vegetative cells in the filaments of
693 *Anabaena* sp PCC 7120. *Cell Microbiol* **13:** 1744-1754

694 Wolk, C.P. (1996) Heterocyst formation. *Annu Rev Genet* **30:** 59–78.

695 Wolk, C.P., and Quine, M.P. (1976) Formation of one-dimensional patterns by stochastic processes and
696 by filamentous blue-green algae. *Dev Biol* **46:** 370–382

697 Xu, X., and Wolk, C.P. (2001) Role for *hetC* in the transition to a nondividing state during heterocyst
698 differentiation in *Anabaena* sp. *J Bacteriol* **183:** 393-396.

699 Yoon, H.S., and Golden, J.W. (1998) Heterocyst pattern formation controlled by a diffusible peptide.
700 *Science* **282:** 935-938.

701 Yoon, H.-S., and Golden, J.W. (2001) PatS and products of nitrogen fixation control heterocyst pattern. *J*
702 *Bacteriol* **183:** 2605–2613.

703

Figure 1. Production of SepJ in *Anabaena* and mutant strains.

(A) Schematics of the C.K1-*sepJ* construct present in plasmid vector pCSAM200 in strains CSDN2a (WT+pSepJ), CSVM20 (Δ*patS*+pSepJ), CSVM21 (Δ*hetN*+pSepJ) and CSDN2b, as indicated. Arrows indicate expression from the C.K1 promoter.

(B) Western blot analysis of SepJ in strains PCC 7120 (WT), CSDN2a (WT+pSepJ) and CSDN2b. The same amount of total protein from membrane fraction preparations was loaded for the three strains, and hybridization with an antibody raised against the SepJ coiled-coil domain was performed as described in Experimental procedures.

(C) Western blot analysis of SepJ in strains CSVT20 (Δ*patS*) and CSVM20 (Δ*patS*+pSepJ), and in strains CSL7 (Δ*hetN*) and CSVM21 (Δ*hetN*+pSepJ). The same amount of total protein from cell extracts was loaded for the four strains, and hybridization with an antibody raised against the SepJ coiled-coil domain was performed as described in Experimental procedures. SepJ levels in Δ*patS*+pSepJ were 2.72-fold higher than in Δ*patS*; levels in Δ*hetN*+pSepJ were 2.67-fold higher than in Δ*hetN* (mean of two independent determinations in each case).

Figure 2. Growth of *Anabaena* and mutant strains.

(A) Filaments of the indicated strains grown in BG11 medium were washed, resuspended in $BG11_0$ medium at 1 μg of Chl ml^{-1}, and 5 μl of successive dilutions were spotted on solid BG11 (containing nitrate) or $BG11_0$ (lacking any source of combined nitrogen) medium. Photographs were taken after 12 days of incubation under growth conditions.

(B) Light micrograph of filaments of *Anabaena* (WT) and strain WT+pSepJ incubated in $BG11_0$ medium for 72 h. The filament suspesions were treated with Alcian blue to stain the heterocyst envelope. The filaments consist of vegetative cells and heterocysts, some indicated by black arrows. A heterocyst doublet can be seen in WT+pSepJ (white arrow). Size bars, 10 μm.

Figure 3. Electron microscopy of portions of filaments of strain WT+pSepJ (A, B, C) and, as a control, *Anabaena* (WT) showing heterocysts (Het) and adjoining vegetative cells.

Filaments grown in BG11 medium were incubated 24 h in $BG11_0$ medium and prepared for electron microscopy as described in Experimental procedures. Three specimens of WT+pSepJ (A, two successive sections; B, one section; C, two sections) and one specimen of WT are shown. Black arrows point to the heterocyst neck. CG, cyanophycin granule. Size bars: 1 µm.

Figure 4. Staining with fluorescent dyes.

(A) Van-FL staining of septal peptidoglycan in wild-type *Anabaena* (WT) and strain WT+pSepJ grown in BG11 medium or incubated in $BG11_0$ medium for 24 h, as indicated. Overlay of cyanobacterial autofluorescence (red) and Van-FL fluorescence (green) is shown. Size bars, 5 µm. Het, heterocyst.

(B) FM 1-43 staining of the cytoplasmic membrane in wild-type *Anabaena* (WT) and strain WT+pSepJ incubated in $BG11_0$ medium for 48 h. Overlay of cyanobacterial autofluorescence (red) and FM 1-43 fluorescence (yellow) is shown. Size bars, 3 µm. Het, heterocyst.

Figure 5. Width of the Van-FL-stained septa between vegetative cells in wild-type *Anabaena* and strain WT+pSepJ.

Filaments from cultures of the indicated strains grown in BG11 medium were washed, resuspended in $BG11_0$ medium and incubated for 24 or 48 hours, as indicated. Filaments were treated with Van-FL and examined by fluorescence microscopy as described in Experimental procedures. The length of the fluorescence signal in the septa between vegetative cells was determined as an indication of septal size. Sizes were grouped in 0.1-µm intervals and their frequencies represented. Figures in squares (red, WT; blue, WT+pSepJ) are mean ± SD expressed in µm. The difference between the mean values in the mutant and wild-type strains was significant in every case (Student's *t* test, $p < 10^{-7}$).

Figure 6. Subcellular localization and distribution of SepJ-GFP in a strain overexpressing SepJ.

(A) Scheme of the *sepJ* genomic region in strain CSDN11 that bears pCSDN11 integrated into the chromosome; note that *sepJ-gfp* is expressed from the *sepJ* promoter whereas *sepJ* is expressed from the C.K3 gene-cassette that bears a strong *psbA* gene promoter.

(B, C) Filaments of strains CSDN11 (*sepJ-gfp*, C.K3-*sepJ* [B]) and CSAM137 (*sepJ-gfp* [C]) from BG11 medium (nitrate-supplemented) cultures were visualized by confocal microscopy. GFP fluorescence is shown in green. Scale bars, 5 μm.

(D) The difference in distribution was analyzed by plotting the fluorescence intensity against the position of the signal at the septum and fitting a Gaussian model to the data for which an example is shown. The Gaussian model equation is given by

$$f(x)=y_0+a*\exp(-0.5*((x-x_0)/b)^2)$$

The definition of the full width at half maximum (FWHM) is shown for CSAM137 with f_{max} being the maximal fluorescence intensity. Following the Gaussian model the FWHM is defined by

$$2\sqrt{2\,ln2}\,b.$$

Figure 7. Visualization of murein sacculi and nasnopores in septal peptidoglycan.

(A) Transmission electron micrograph of a murein sacculus corresponding to 11 cell units isolated from *Anabaena*.

(B) Sacculus corresponding to three cell units illustrating septal peptidoglycan disks (arrows).

(C) Septal peptidoglycan disks from *Anabaena* (WT) and WT+pSepJ illustrating the presence of nanopores. All sacculi are from filaments grown in BG11 medium.

Figure 8. Heterocyst pattern in wild-type *Anabaena* and mutant strains.

Filaments of the indicated strains from BG11 medium were washed with $BG11_0$ medium, resuspended in $BG11_0$ medium and incubated for 24 or 48 hours, as indicated. Cells were counted after staining with Alcian Blue. 117 to 252 intervals (except for CSVM21 at 24 h, 20 intervals) were counted. Interval zero corresponds to contiguous heterocysts.

794 Table 1. Intercellular transfer of calcein and 5-carboxyfluorescein (5-CF) in WT+pSepJ
795 and *Anabaena* (WT).

Measurement (number of replicates)	Calcein	5-CF
	***R* [s^{-1}] (± SD)**	***R* [s^{-1}] (± SD)**
1. Vegetative cells in presence of nitrate		
a) WT (35/41)	0.083 ± 0.032	0.133 ± 0.049
b) WT+pSepJ (34/18)	0.075 ± 0.031	0.110 ± 0.052
2. Vegetative cells 48 h after nitrogen deprivation		
a) WT (21/19)	0.102 ± 0.025	0.101 ± 0.052
b) WT+pSepJ (24/18)	0.109 ± 0.039	0.094 ± 0.033
3. Heterocysts 48 h after nitrogen deprivation		
a) WT (15/5)	0.022 ± 0.013	0.027 ± 0.012
b) WT+pSepJ (10/10)	* 0.038 ± 0.021	0.030 ± 0.024

796

797 Student's *t*-tests show that *R* is significantly different for calcein between (3a) and (3b)
798 (p = 0.021), marked with an asterisk. No significant differences were detected for
799 calcein or 5-CF between (1a) and (1b) or (2a) and (2b), as well as for 5-CF between (3a)
800 and (3b).

801

Table 2. Heterocyst pattern in wild-type *Anabaena* and mutant strains.

Strain	Genotype	24 h without combined N			48 h without combined N		
		Heterocysts (%)	Mean interval size (cells)	Heterocyst doublets (%)	Heterocysts (%)	Mean interval size (cells)	Heterocyst doublets (%)
PCC 7120	WT	7.4 ± 2.0	13.2 ± 3.9	0	12.1 ± 2.4	13.2 ± 4.7	1.5
WT+pSepJ	PCC 7120 (pCSAM200::C.K1-*sepJ*)	5.0 ± 1.6 (0.002)	18.0 ± 7.8 ($<10^{-3}$)	3.8 (N.A.)	8.3 ± 1.6 (0.001)	11.0 ± 4.1 ($<10^{-3}$)	8.4 ($<10^{-3}$)
CSVT20	Δ*patS*	15.4 ± 2.3	9.4 ± 3.8	13.4	17.9 ± 2.2	9.5 ± 4.3	13.2
Δ*patS*+pSepJ	CSVT20 (pCSAM200::C.K1-*sepJ*)	16.3 ± 3.3 (0.482)	8.8 ± 3.9 (0.206)	19.8 ($<10^{-3}$)	22.3 ± 8.0 (0.213)	8.3 ± 5.1 (0.028)	23.4 ($<10^{-3}$)
CSL7	Δ*hetN*	11.5 ± 1.3	10.8 ± 3.3	6.8	13.5 ± 1.9	10.2 ± 4.6	16.2
Δ*hetN*+pSepJ	CSL7 (pCSAM200::C.K1-*sepJ*)	2.9 ± 1.4 ($<10^{-3}$)	15.4 ± 5.0 ($<10^{-3}$)	10.0 ($<10^{-3}$)	10.2 ± 3.1 (0.077)	10.1 ± 4.0 (0.887)	14.0 (0.348)

Filaments from BG11-grown cultures were incubated in $BG11_0$ medium (without combined N) for 24 or 48 h, and samples were taken and stained with Alcian blue to facilitate the identification of heterocysts. Heterocysts and vegetative cells from two to four different cultures from each strain and time of incubation were counted. % Hets, percentage of heterocysts ± SD of the mean in 4 to 14 different microscopy fields; 106 to 576 cells, including heterocysts that were separated from filaments, were counted per field. Interval size refers to the number of vegetative cells between heterocysts, which could be determined only in filaments containing at least two heterocysts (117 to 252 intervals were counted for each strain and incubation time, except for Δ*hetN*+pSepJ at 24 h, 20 intervals). Mean interval size (± SD) corresponds to intervals ≥ 1 vegetative cell, and percentage of heterocyst doublets corresponds to the percentage of interval sizes with a value of 0 (both parameters were deduced from the same data represented in Fig. 8). For the percentage of heterocysts and mean interval size, the Student's *t* test *p* value for the comparison of each SepJ-overproducing strain and its parental strain is indicated in parenthesis. For the percentage of heterocyst doublets, the actual figures were classified into two categories (interval = 0; interval > 0), and the distribution in each SepJ-overproducing strain was compared to that in its parental strain using the X^2 test (*p* given in parenthesis). N.A., not applicable because of a zero value in the wild type.

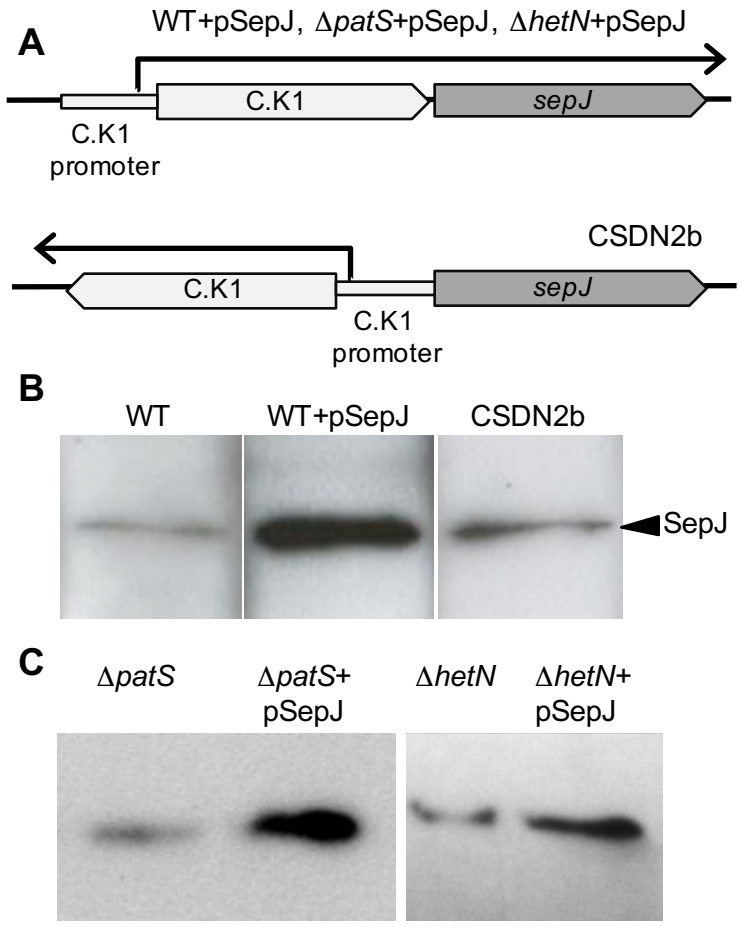
A
WT+pSepJ, ΔpatS+pSepJ, ΔhetN+pSepJ
C.K1
sepJ
C.K1
promoter
CSDN2b
C.K1
sepJ
C.K1
promoter
B
WT
WT+pSepJ
CSDN2b
SepJ
C
ΔpatS
ΔpatS+
pSepJ
ΔhetN
ΔhetN+
pSepJ

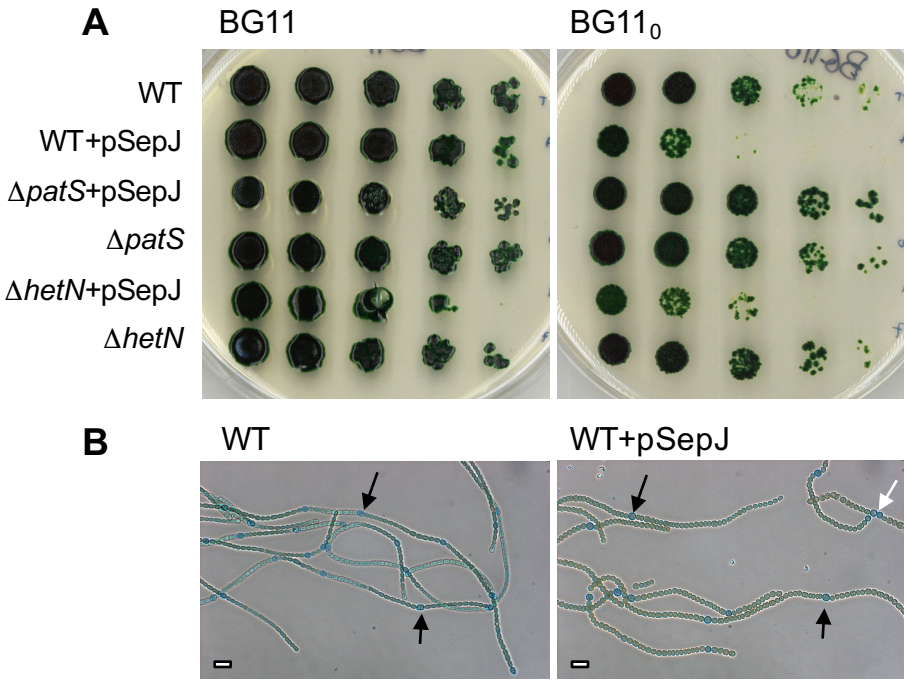
A
BG11
BG11$_0$
WT
WT+pSepJ
Δ*patS*+pSepJ
Δ*patS*
Δ*hetN*+pSepJ
Δ*hetN*
B
WT
WT+pSepJ

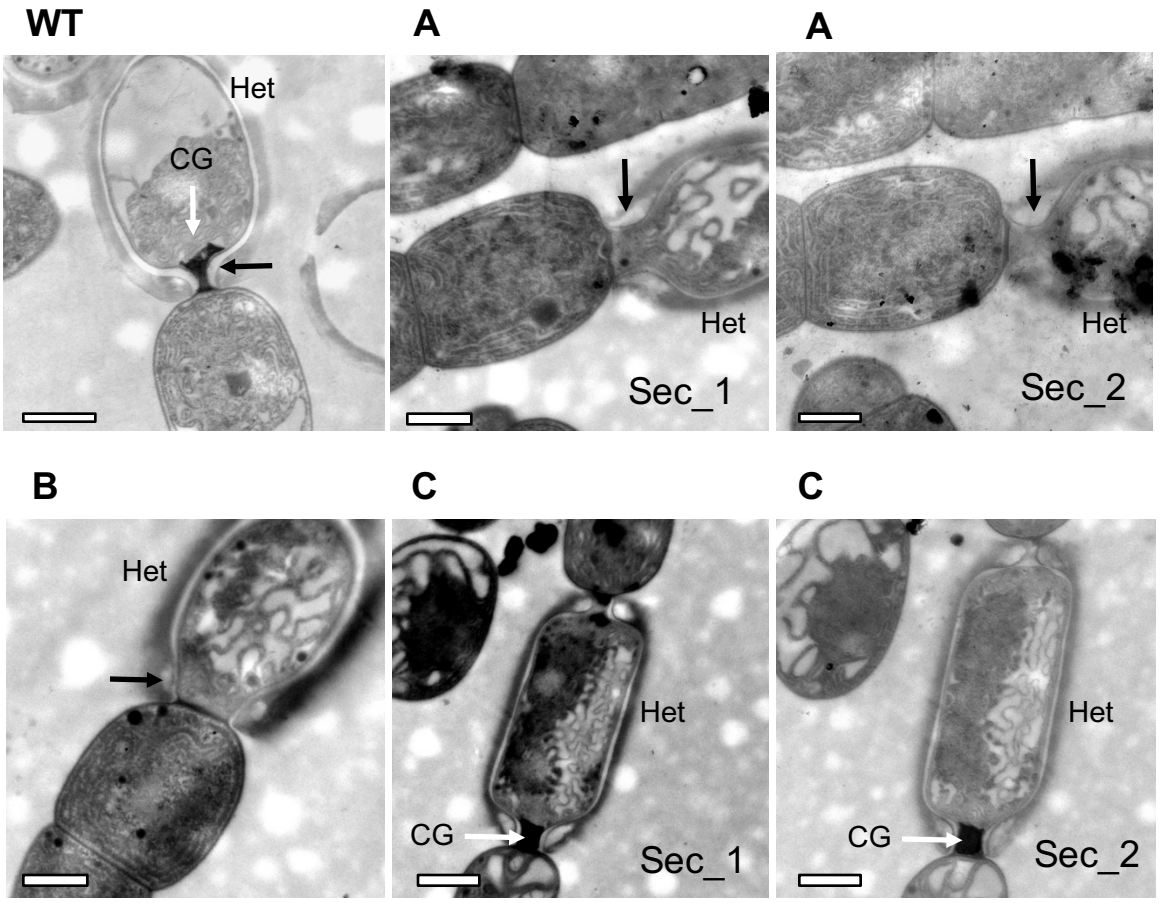
WT
Het
CG
A
Het
Sec_1
A
Het
Sec_2
B
Het
C
Het
CG
Sec_1
C
Het
CG
Sec_2

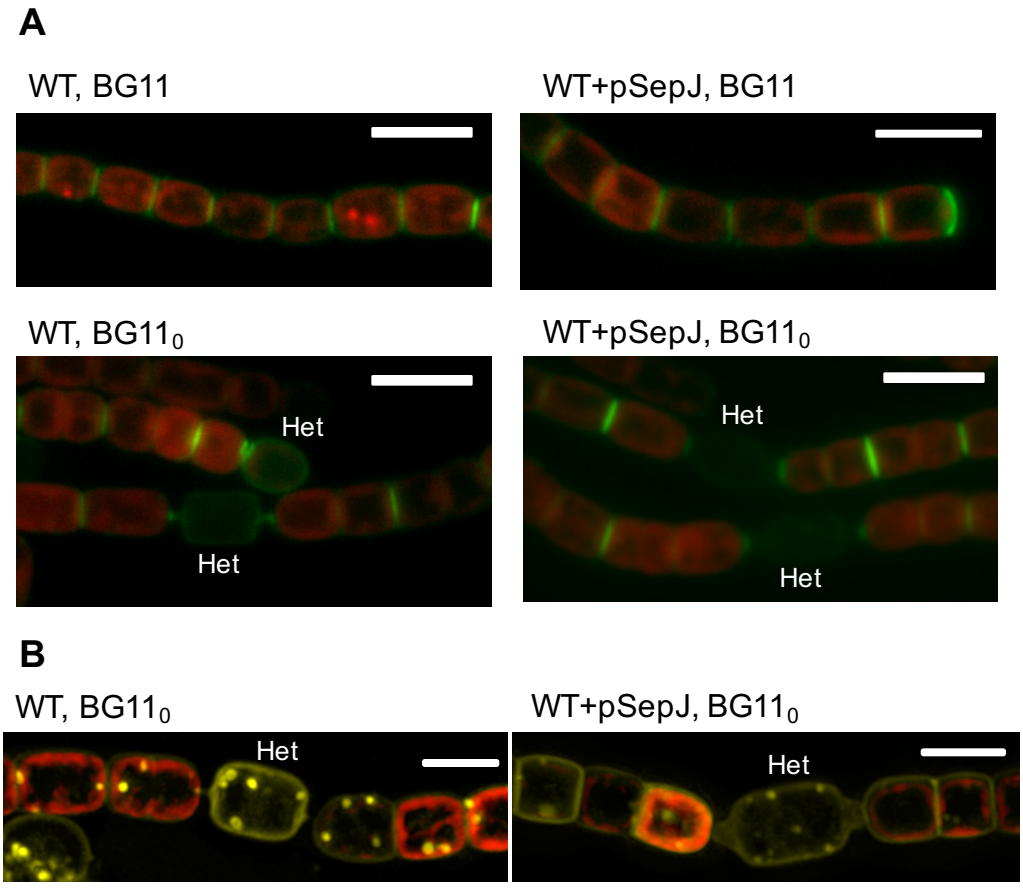
A
WT, BG11
WT+pSepJ, BG11
WT, BG11$_0$
WT+pSepJ, BG11$_0$
Het
Het
Het
Het
B
WT, BG11$_0$
WT+pSepJ, BG11$_0$
Het
Het

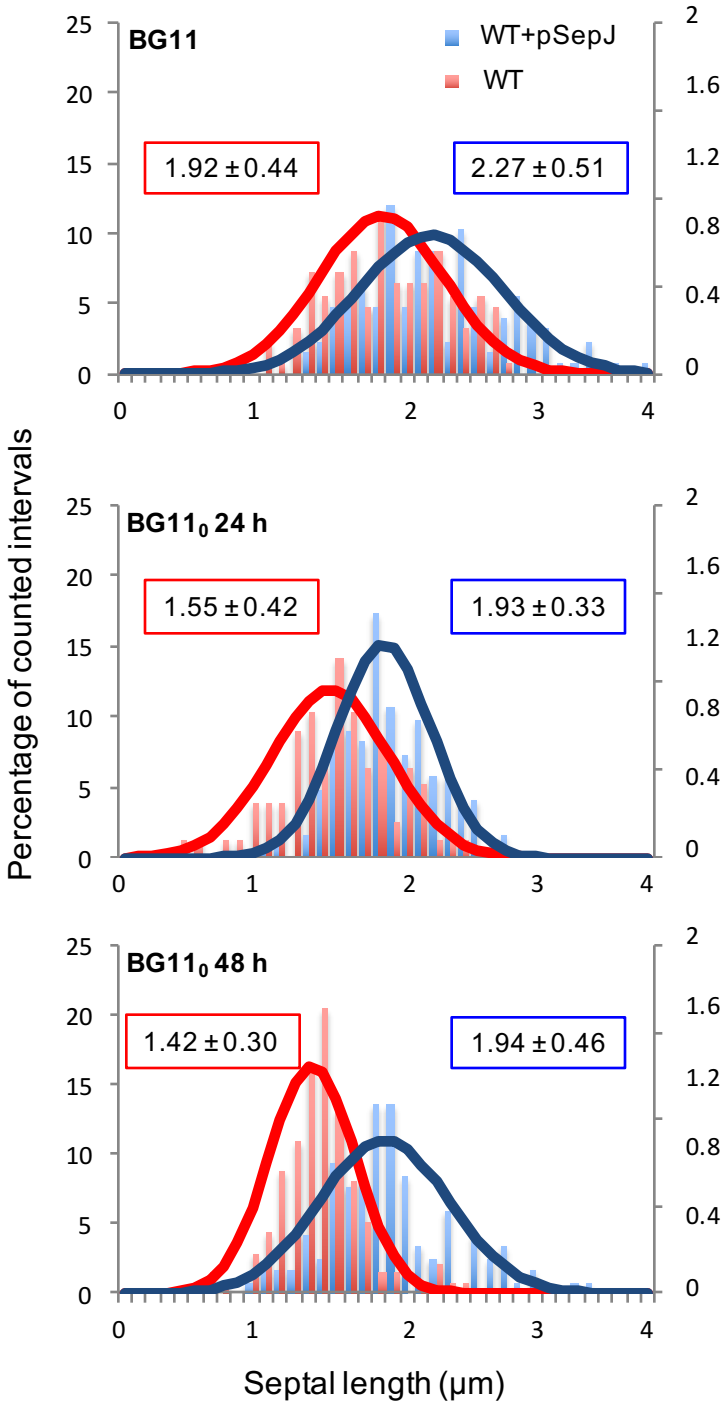
BG11
WT+pSepJ
WT
1.92 ± 0.44
2.27 ± 0.51
BG11$_0$ 24 h
1.55 ± 0.42
1.93 ± 0.33
BG11$_0$ 48 h
1.42 ± 0.30
1.94 ± 0.46
Percentage of counted intervals
Septal length (μm)

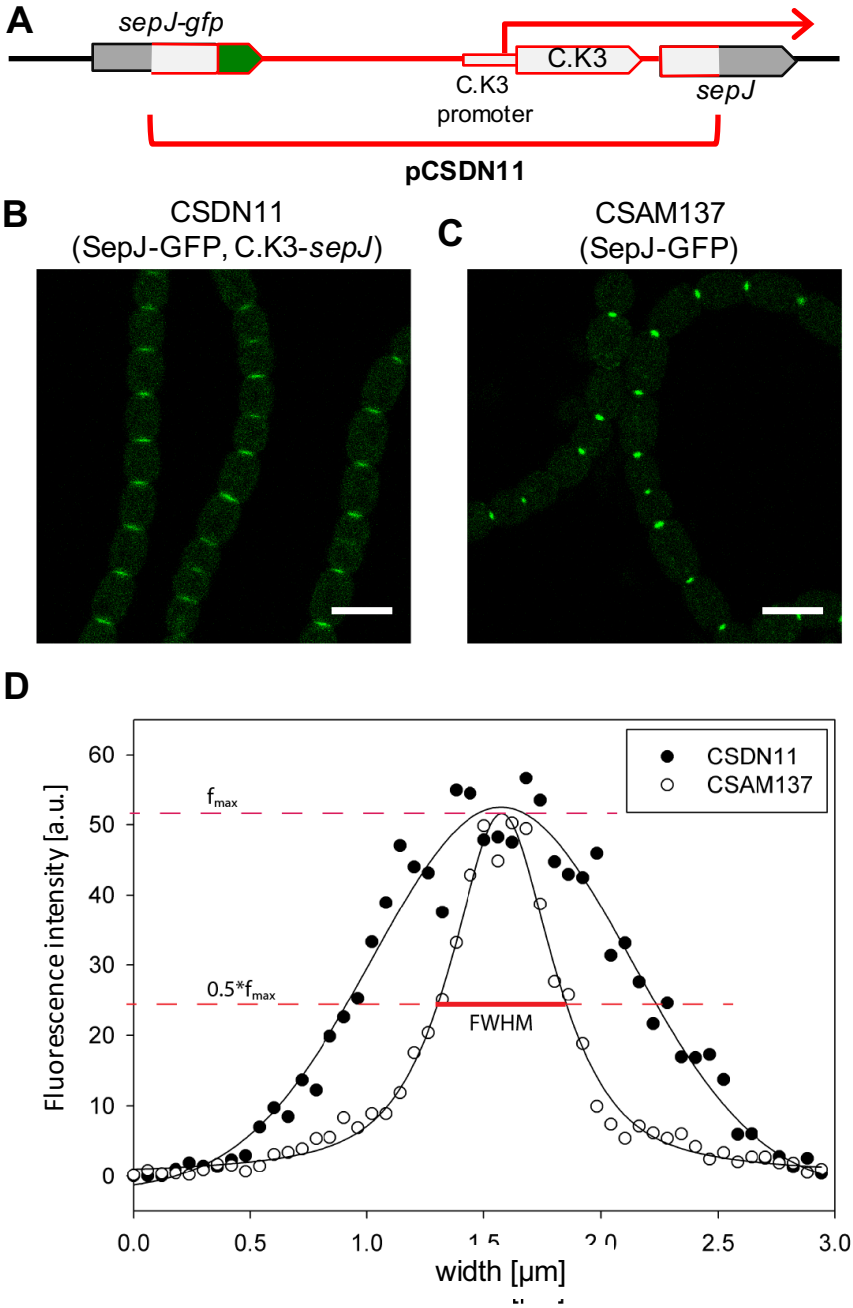
A
sepJ-gfp
C.K3
C.K3
promoter
sepJ
pCSDN11
B
CSDN11
(SepJ-GFP, C.K3-sepJ)
C
CSAM137
(SepJ-GFP)
D
CSDN11
CSAM137
fmax
0.5*fmax
FWHM
Fluorescence intensity [a.u.]
width [µm]
0
10
20
30
40
50
60
0.0
0.5
1.0
2.5
3.0

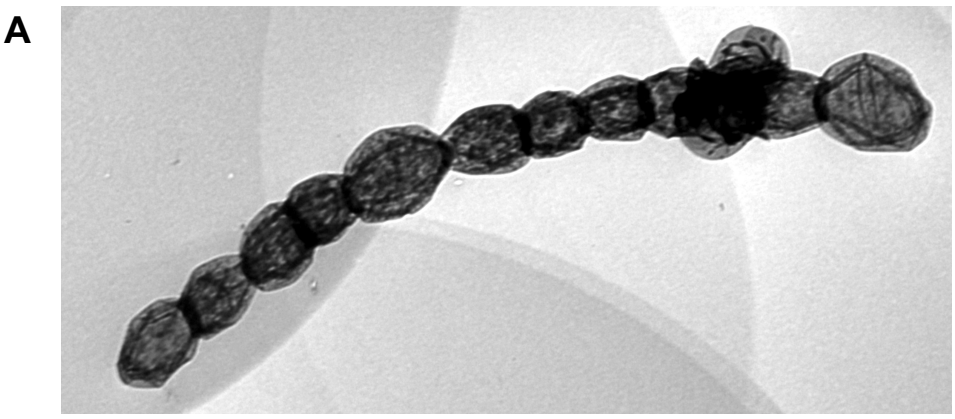
A

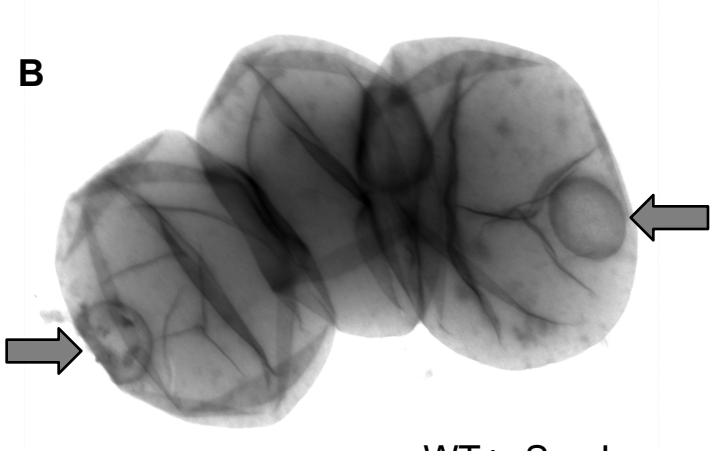
B

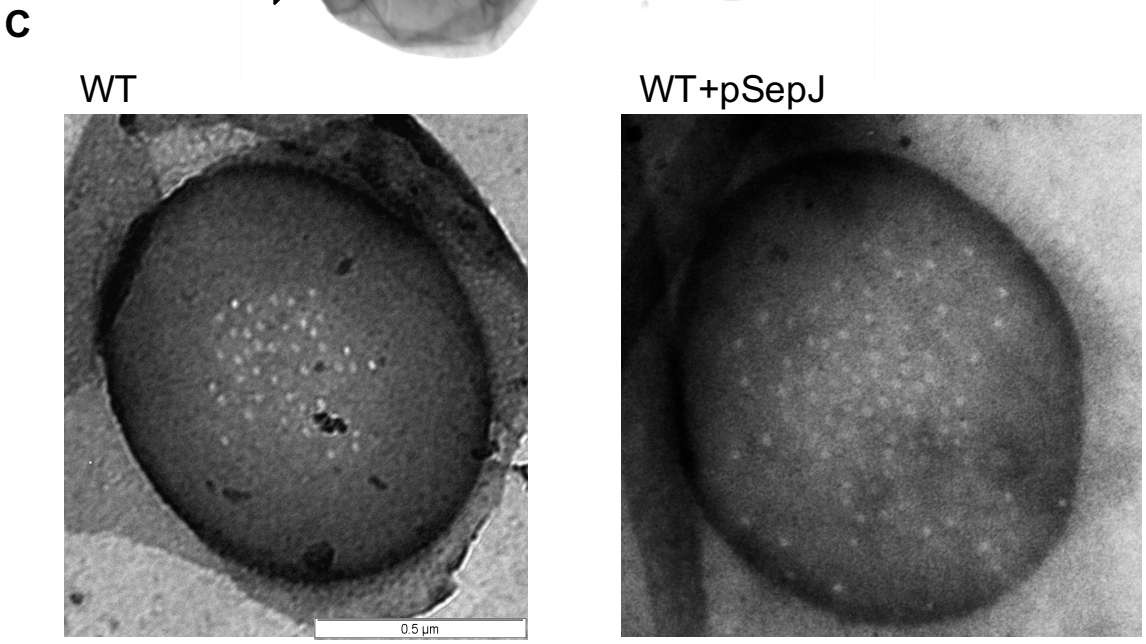
C
WT
WT+pSepJ
0.5 µm

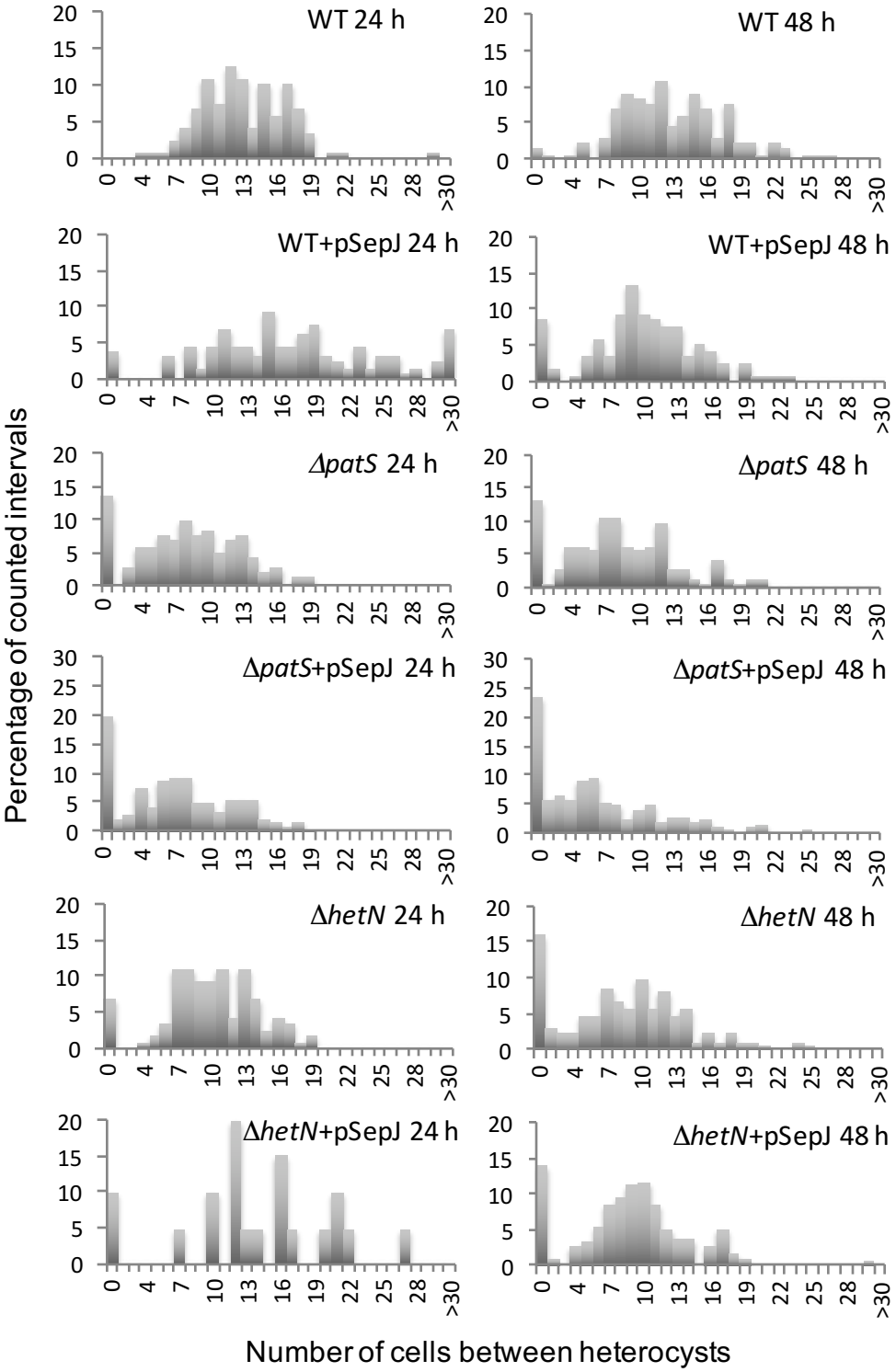
WT 24 h
WT 48 h
WT+pSepJ 24 h
WT+pSepJ 48 h
ΔpatS 24 h
ΔpatS 48 h
ΔpatS+pSepJ 24 h
ΔpatS+pSepJ 48 h
ΔhetN 24 h
ΔhetN 48 h
ΔhetN+pSepJ 24 h
ΔhetN+pSepJ 48 h
Percentage of counted intervals
Number of cells between heterocysts

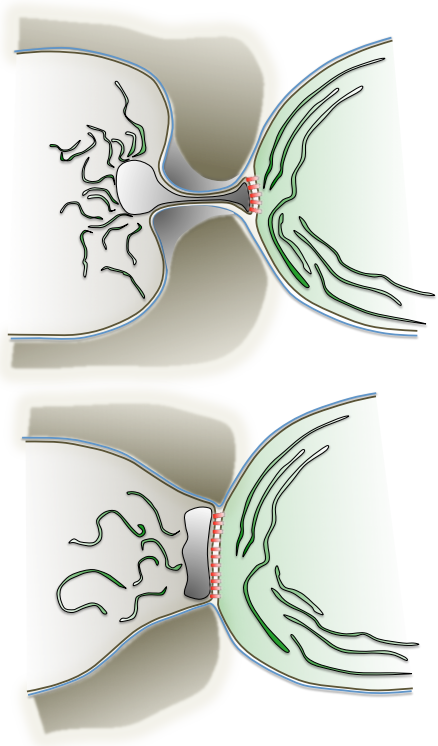

Abbreviated Summary

Overexpression of septal protein SepJ in the filamentous, heterocyst-forming cyanobacterium *Anabaena* alters the structure of the intercellular septa and the heterocyst pattern regulated by the PatS morphogen and a HetN-related signal. The drawings show parts of a heterocyst and adjacent vegetative cell in wild-type *Anabaena* (upper panel) and the SepJ overexpressing strain (lower panel). Note the different sizes of the septum in the two strains and the possible presence of a higher number of SepJ-related septal junctions (red lines) in the SepJ overexpressing strain than in the wild type.

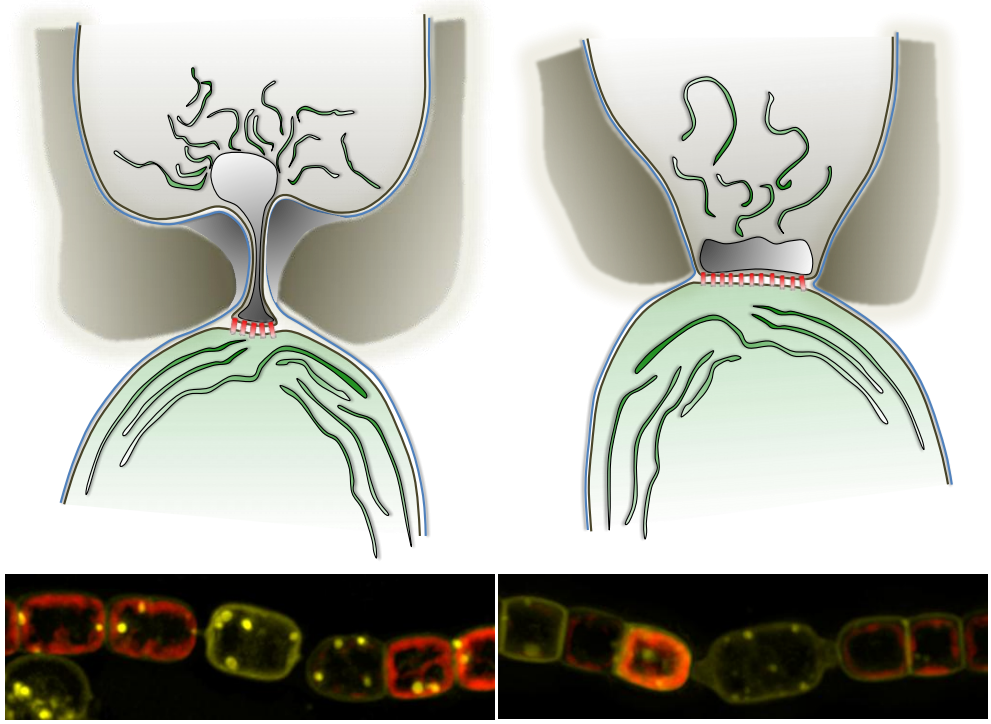

An intercellular exchange of regulators and nutrients takes place through septal junctions in the filament of heterocyst-forming cyanobacteria. The effect of overexpression of SepJ, a putative septal junction protein, was investigated in this work.